

## PLATELETS AND THROMBOPOIESIS

## Platelet amyloid precursor protein is a modulator of venous thromboembolism in mice

Ilaria Canobbio,<sup>1,\*</sup> Caterina Visconte,<sup>1,\*</sup> Stefania Momi,<sup>2</sup> Gianni Francesco Guidetti,<sup>1</sup> Marta Zarà,<sup>1</sup> Jessica Canino,<sup>1</sup> Emanuela Falcinelli,<sup>2</sup> Paolo Gresele,<sup>2</sup> and Mauro Torti<sup>1</sup>

<sup>1</sup>Department of Biology and Biotechnology, University of Pavia, Pavia, Italy; and <sup>2</sup>Department of Internal Medicine, University of Perugia, Perugia, Italy

## Key Points

- APP is dispensable for platelet activation and arterial thrombosis.
- APP is an important novel regulator of vein thrombosis and controls coagulation and neutrophil extracellular traps formation.

The amyloid precursor protein (APP), primarily known as the precursor of amyloid peptides that accumulate in the brain of patients with Alzheimer disease, is abundant in platelets, but its physiological function remains unknown. In this study, we investigated the role of APP in hemostasis and thrombosis, using APP knockout (KO) mice. *Ex vivo* aggregation, secretion, and integrin  $\alpha$ IIb $\beta$ 3 inside-out activation induced by several agonists were normal in APP-deficient platelets, but the number of circulating platelets was reduced by about 20%, and their size was slightly increased. Tail bleeding time was normal, and *in vivo*, the absence of APP did not alter thrombus formation in the femoral artery. In contrast, in a model of vein thrombosis induced by flow restriction in the inferior vena cava, APP-KO mice, as well as chimeric mice with selective deficiency of APP in blood cells, developed much larger thrombi than control animals, and were more sensitive to embolization. Consistent with this, in a pulmonary thromboembolism model, larger vessels were occluded. APP-KO mice displayed a shorter APTT, but not PT, when measured in the presence of platelets. Moreover, the activity of factor XIa (FXIa), but not FXIIa, was higher in APP-KO mice compared with controls. APP-KO mice presented a higher number of circulating platelet-leukocyte aggregates, and neutrophils displayed a greater tendency to protrude extracellular traps, which were more strongly incorporated into venous thrombi. These results indicate that platelet APP limits venous thromboembolism through a negative regulation of both fibrin formation and neutrophil function. (*Blood*. 2017;130(4):527-536)

## Introduction

Amyloid precursor protein (APP) is a type I transmembrane glycoprotein primarily known as the metabolic precursor of amyloid A $\beta$  peptides, whose accumulation in brain parenchyma and cerebral vessel walls is correlated with the onset of Alzheimer disease.<sup>1</sup> Membrane APP can be proteolytically processed by 2 alternative pathways. The combined action of  $\beta$ - and  $\gamma$ -secretases releases amyloidogenic A $\beta$  peptides, whereas the alternative action of  $\alpha$ -secretase releases a larger soluble fragment, sAPP $\alpha$ , and prevents subsequent A $\beta$  generation by  $\gamma$ -secretase.<sup>2</sup> Probably because of this complex and typically very rapid proteolytic processing, the physiological function of APP is still poorly understood. The full-length protein possesses a number of biologically active domains, suggesting its involvement in diverse physiological processes, including cell adhesion and activation.<sup>3</sup> Studies with transfected cell lines as well as knockout (KO) mice have actually implicated APP in cell proliferation, neurite outgrowth, and synaptogenesis.<sup>4</sup>

APP is also expressed in extraneuronal tissues and is particularly abundant in platelets,<sup>5</sup> with a total number of 9300 copies/platelet, as estimated by a recent proteomic study.<sup>6</sup> Alternative splicing of the APP gene generates multiple isoforms. The APP isoforms expressed in platelets (APP751 and APP770), but not the shorter isoform expressed in neurons (APP695), contain an additional domain in the extracellular region, which is structurally and functionally related to the Kunitz-type

serine proteinase inhibitors (KPIs).<sup>7-9</sup> Only about 10% of the total platelet APP is expressed as an intact glycoprotein on the plasma membrane. The majority of APP is cleaved into proteolytic soluble fragments that are stored in  $\alpha$ -granules.<sup>7,10</sup> Platelets contain  $\alpha$ ,  $\beta$ , and  $\gamma$  secretases, and therefore metabolize APP through both nonamyloidogenic and amyloidogenic pathways.<sup>11</sup> Platelets are considered the main source of A $\beta$  in plasma, and there is evidence that, through A $\beta$  production, platelets participate in the onset and progression of Alzheimer disease.<sup>12</sup> Conversely, A $\beta$  peptides are capable of triggering platelet activation and adhesion, thus promoting thrombotic events.<sup>13-15</sup>

Under physiological conditions, however, the majority of APP is processed by the nonamyloidogenic pathway, and  $\alpha$ -secretase is activated by a Ca<sup>2+</sup>/calmodulin-dependent mechanism on platelet activation.<sup>10,16</sup> Platelet secretion and the shedding of membrane APP from platelets release KPI-containing soluble fragments that inhibit the activity of coagulation factors. Actually, these soluble APP fragments were originally identified as the cell-secreted proteinase inhibitor nexin-2, and were demonstrated *in vitro* to be effective inhibitors of the coagulation FXa, FIXa, FXIa, and FVIIa:tissue factor complex.<sup>9,17-20</sup> *In vivo* studies on APP-KO mice have indicated that, as a result, APP negatively controls cerebral thrombosis.<sup>21,22</sup> Nevertheless, a thorough investigation of the contribution of platelet-derived

Submitted 26 January 2017; accepted 8 June 2017. Prepublished online as *Blood* First Edition paper, 13 June 2017; DOI 10.1182/blood-2017-01-764910.

\*I.C. and C.V. contributed equally to this study.

The publication costs of this article were defrayed in part by page charge payment. Therefore, and solely to indicate this fact, this article is hereby marked "advertisement" in accordance with 18 USC section 1734.

© 2017 by The American Society of Hematology

APP in platelet function and its implications in peripheral arterial and vein thrombosis is still missing.

In this study, we used APP KO mice to demonstrate an important role for platelet APP in limiting deep vein thrombosis by multiple mechanisms involving both inhibition of the intrinsic pathway of coagulation and the prevention of neutrophil extracellular traps (NETs) formation.

## Methods

### Chemicals and reagents

Fluorescein isothiocyanate-conjugated anti-CD41 and peridinin chlorophyll protein complex-conjugated anti-CD45 were from Biolegend. Antibodies against P-selectin, GPVI, CD42b, CD41, CD49b, AlexaFluor488-conjugated anti-GPIX (clone Xia.B4), and phycoerythrin-conjugated anti-GPIb $\alpha$  (clone Xia.G5) were from Emfret Analytics. Fluorescein isothiocyanate-fibrinogen was from Molecular Probes. Monoclonal antibodies against APP (22C11) and tubulin (DM1A) were from Chemicon and Santa Cruz Biotechnology, respectively. Antibody against citrullinate histone H3 (cit-H3) was from Abcam, and anti-cathelicidin-related antimicrobial peptide (CRAMP) antibody was from Innovagen. Reagents for activated partial thromboplastin time (APTT), prothrombin time (PT), fibrinogen, and coagulation factors were from Instrumentation Laboratories. All other reagents were from Sigma Aldrich. APP KO mice in a C57BL/6J background were generated as described previously,<sup>23</sup> and kindly provided by U. Muller (University Heidelberg, Germany). All the mice used were 4 to 6 months of age (average weight, 25–30 g) and balanced for sex distribution. Age-matched C57BL/6J wild-type (WT) mice were used as control. All the procedures involving the use of mice were approved by the Committees on Ethics of Animal Experiments of the Universities of Pavia and Perugia and by the Italian Ministry of Public Health (authorization protocol numbers 74/2007, 76/2007-B, and 561/2015-PR).

### Platelet preparation and analyses

Mouse platelet isolation and platelet and white cell count in whole blood were performed as previously described.<sup>24</sup> Analysis of glycoprotein expression by flow cytometry and by immunoblotting, platelet morphology by electron microscopy, platelet secretion as P-selectin exposure, integrin  $\alpha$ Ib $\beta$ 3 activation as fibrinogen binding, and agonist-induced aggregation were performed as previously described.<sup>25</sup>

### Determination of platelet life span

Platelet clearance in vivo was determined essentially as previously described.<sup>26</sup> Briefly, platelets were labeled in vivo by intravenous injection of 5  $\mu$ g Alexa Fluor 488-conjugated anti-GPIX antibody. Whole blood (40  $\mu$ L) was drawn every 24 hours on injection and incubated with PE-conjugated antibody to GPIb $\alpha$  for 10 minutes. Samples were analyzed by flow cytometry and the ratio of Alexa Fluor 488-positive to PE-positive platelets was determined. Five mice of each genotype were used for these experiments.

### Megakaryocyte isolation

Bone marrow cells were flushed from femurs and tibias and cultured for 5 days in the presence of 10 ng/mL thrombopoietin. Megakaryocytes were recovered by centrifugation on 1.5% to 3% bovine serum albumin gradient. For evaluation of proplatelet formation,  $1 \times 10^5$  cells were seeded onto glass coverslips coated with 100  $\mu$ g/mL fibrinogen for 6 hours at 37°C. Cells were then fixed with 2% paraformaldehyde, permeabilized with 0.25% Triton X-100, and stained with anti-tubulin antibody (1:500) for 1 hour at room temperature, followed by incubation with AlexaFluor488-conjugated secondary antibody. Nuclear counterstaining was performed with Hoechst 33258 (100 ng/mL). The coverslips were mounted onto glass slides with ProLong Gold antifade reagent and images acquired by an Olympus BX51 microscope (Olympus), using a 20 $\times$ /0.5 UPlanF1 objective. Megakaryocytes protruding proplatelets were counted in 20 fields and expressed as percentage on the total number of megakaryocytes.

### Tail bleeding time and blood loss

Tail bleeding time and quantification of blood loss were measured in 8 WT and 11 APP-KO mice, essentially as previously described.<sup>27,28</sup>

### Platelet pulmonary thromboembolism

Thrombin-induced pulmonary thromboembolism was carried out on groups of 8 mice for each genotype on injection of 500 U/kg thrombin into a tail veins, as previously described.<sup>29</sup>

### Femoral artery thrombosis

Photochemical-induced femoral artery thrombosis was induced in anesthetized mice, as previously described.<sup>30</sup> Six WT and 6 APP-KO mice were used for these experiments.

### Inferior vena cava ligation

Inferior vena cava (IVC) ligation was obtained as previously described.<sup>31,32</sup> Briefly, mice were anesthetized with xylazine (5 mg/kg) and ketamine (50 mg/kg) and placed in a supine position. After laparotomy, intestines were exteriorized, and sterile saline was applied during the whole procedure to prevent drying. After gentle separation from the aorta, IVC was ligated by a 7.0 polypropylene suture immediately below the renal veins (toward the tail) over a 30-gauge needle, and then the needle was removed to obtain a partial flow restriction. The side and back branches of IVC were not ligated. The needle was placed outside the vessel so that piercing or any other injury to the IVC wall was completely avoided. After surgery, peritoneum and skin were closed by monofilament absorbable suture and 6.0 silk, respectively. Mice were killed after 24 or 48 hours, and thrombi developed in the IVC below the suture (toward the tail) were taken for analysis. Thrombus weight and thrombus length were measured. A total of 27 WT and 27 APP-KO mice were used for these experiments.

### Bone marrow cell transplantation

Generation of chimeric mice was performed essentially as described.<sup>27</sup> Briefly, bone marrow cells were harvested from the femurs and tibias of donor WT and APP-KO mice. Then,  $1 \times 10^7$  cells (in 300  $\mu$ L) from APP-KO bone marrows were transplanted by intravenous injection into irradiated recipient WT animals. Control experiments were performed by transplanting bone marrow from WT donors into irradiated WT recipient mice. Six WT/WT and 6 WT/APP-KO chimeric mice were generated.

### Blood clotting assays

Blood was collected with 3.8% sodium citrate and centrifuged for 10 minutes at  $180 \times g$  to obtain platelet-rich plasma (PRP). PRP was centrifugated for 10 minutes at  $18000 \times g$  at 4°C to obtain platelet-poor plasma (PPP). PPP and PRP were tested as indicated. APTT and PT were measured by standard assays in an automatic coagulometer (ACL 300R; Instrumentation Laboratory), using the Instrumentation Laboratory kits, according to the manufacturer's instructions. Plasma fibrinogen was measured by the Clauss method in a Coagulab MJ coagulometer (Ortho Diagnostic Systems), using bovine thrombin. Plasma levels of FXIIa and FXIa were assayed by 1-stage clotting methods, using commercially available human plasmas deficient in the respective coagulation factor.<sup>27,33</sup>

### Neutrophil isolation and analysis of NETs formation

Neutrophils were isolated as described,<sup>34</sup> with minor modifications. Mice were killed, and bone marrow cells were flushed in RPMI medium supplemented with 10% fetal bovine serum and 1% penicillin/streptomycin. The cell suspension was filtered with 70  $\mu$ m cell strainer, centrifugated ( $400 \times g$  for 7 minutes), resuspended in hypotonic buffer for red blood cells lysis, and centrifugated again at  $400 \times g$  for 7 minutes. Finally, the cell pellet was resuspended in 1 mL Ca-Mg-free HBSS and centrifugated on 62.5% Percoll for 30 minutes at  $1000 \times g$  at room temperature. Typically,  $1-2 \times 10^6$  bone marrow-derived neutrophils were harvested per mouse.

Neutrophils ( $3 \times 10^5$  cells) were left untreated or stimulated with phorbol-12-myristate-13-acetate (PMA) (100 nM) for 3 hours or by addition of platelets ( $1 \times 10^8$  platelets) for 30 minutes before plating onto glass coverslips on 12-well plates. The plate was cytospun, and adherent cells were fixed with 2% paraformaldehyde and permeabilized with ice-cold 0.25% Triton-X-100. For immunofluorescence labeling of NETs, cells were stained for Cit-H3 (1:500 dilution) and counterstained for DNA with Hoechst 33342 (1:1000 dilution), essentially as described.<sup>35</sup>

Analysis of NETs inclusion into venous thrombi was performed by the adaptation of the protocol described by Knight et al,<sup>36</sup> using specific antibodies against the NET-related markers CRAMP and Cit-H3, and horseradish peroxidase-conjugated secondary antibodies combined with diaminobenzidine tetrahydrochloride substrate reaction.

### Data and statistical analysis

The reported figures are representative of at least 3 different experiments. Statistical analysis was performed using Prism Version 4 software (GraphPad), and data were compared by unpaired *t* test. Data are reported as mean  $\pm$  standard error of the mean (SEM).

## Results

### The lack of APP is associated with a mild macrothrombocytopenia in mice

APP-KO mice are viable, fertile, and in an overall good health status and do not manifest any evident bleeding. Immunoblotting analysis confirmed the absence of APP in platelets from KO mice (Figure 1A), whereas flow cytometry studies demonstrated that the expression of other major membrane glycoproteins, including integrin  $\alpha$ IIB $\beta$ 3 (CD41/CD61), integrin  $\alpha$ 2 (CD49b), GPIIb $\alpha$  (CD42b), GPV, GPVI, and CD9, was comparable to that observed in control WT platelets (Figure 1B). The number of circulating platelets was slightly but significantly lower in APP-KO compared with WT mice ( $818 \pm 88 \times 10^3/\mu\text{L}$  vs  $1095 \pm 73 \times 10^3/\mu\text{L}$ ;  $P < .05$ ), whereas the number of leukocytes was comparable in the 2 genotypes (Figure 1C). The life span of circulating platelets was not altered in the absence of APP (Figure 1D), indicating that the reduced platelet count in the APP-KO mice was not the result of a faster removal. Electron microscopy showed an overall normal platelet morphology, with a comparable number of  $\alpha$  and  $\delta$  granules in WT and APP-KO mice (Figure 1E). However, accurate measurement of the platelet diameter revealed that platelets from APP-KO mice were larger than those from control littermates ( $2.74 \pm 0.29 \mu\text{m}$  vs  $1.84 \pm 0.22 \mu\text{m}$ ;  $P < .05$ ). These results suggest a possible alteration of platelet formation in the absence of APP. In this regard, we found that although the number of mature megakaryocytes differentiated from bone marrow cells was comparable in WT and APP-KO mice, APP-deficient megakaryocytes showed a greater propensity in protruding proplatelets, suggesting that APP may regulate platelet release (Figure 1F).

### Platelet activation, secretion, and aggregation are normal in APP-KO mice

To investigate the role of APP in platelet function, we measured ex vivo aggregation of washed platelets stimulated with different doses of the most common soluble agonists, including TRAP4, U46619, convulxin, and ADP. The representative traces reported in Figure 2A show that, under all the conditions analyzed, no differences in platelet aggregation were observed between APP-KO and WT platelets. Inside-out activation of integrin  $\alpha$ IIB $\beta$ 3, measured as binding of labeled fibrinogen, was comparable in platelets from the 2 genotypes (Figure 2B). Moreover, no differences in agonist-induced P-selectin exposure were

observed (Figure 2C), indicating that secretion occurred normally in the absence of APP. Thus, these results suggest that the lack of APP does not significantly affect the major platelet responses ex vivo. The overall hemostatic process in WT and KO mice was assessed by comparing tail bleeding time. Figure 2D shows that the time required for bleeding cessation, as well as the amount of blood lost (as amount of hemoglobin), was not affected by the absence of APP.

### APP negatively controls venous, but not arterial, thrombosis

We next investigated whether APP contributes to thrombus formation. Previous studies have reported a role for APP in regulating cerebral thrombosis.<sup>21,22</sup> Here, we performed in vivo studies to investigate the involvement of APP in peripheral arterial and in IVC thrombosis. Femoral artery thrombosis was analyzed using a model of photochemical-induced lesion in mice infused with rose Bengal by measuring the blood flow in the exposed artery with a laser Doppler probe. Figure 3A shows that the time for complete artery occlusion and blood flow cessation was comparable in WT and APP-KO mice, indicating peripheral artery thrombosis is not significantly affected by the lack of APP.

Deep vein thrombosis (DVT) was evaluated in the IVC on blood flow reduction caused by vessel narrowing through the application of a ligature.<sup>31,32</sup> After 24 and 48 hours, animals were killed, and the formed thrombi were isolated, measured, and weighted. Figure 3B shows that APP-KO mice developed much larger thrombi than WT mice, with a significant increase of both the length and the weight of venous thrombi both after 24 and 48 hours. After 48 hours from IVC ligation, thrombi were reduced in size in both genotypes, likely as a consequence of embolization. In fact, staining of lung sections with phosphotungstic acid-hematoxylin to reveal fibrin deposits showed that 48 hours after IVC ligation, a greater percentage of vessels was occluded in APP-KO compared with WT mice (Figure 3C). Moreover, we observed 3 cases of death out of 14 APP-KO mice, but only 1 among the 13 WT mice analyzed.

To confirm that the protection from venous thrombosis is provided by APP expressed in platelets, we generated chimeric mice by transplantation of bone marrow cells from APP-KO mice into recipient WT mice. Although the size and weight of venous thrombi were overall reduced in the chimeric mice, Figure 3D shows that when WT mice were transplanted with APP-deficient blood cells, the thrombi formed within 24 hours of IVC ligation were still significantly bigger than those observed in transplanted control mice. These results outline the importance of blood cell-derived APP in the control of venous thrombosis.

The greater tendency of APP-KO mice to develop vein thrombosis was confirmed by the analysis of pulmonary thromboembolism. Histological analysis of lung sections revealed that although the number of occluded vessels was not significantly different between the 2 genotypes (Figure 4), their average diameter was significantly larger in APP-KO mice than in WT animals (Figure 4), indicating the formation of bigger clots in the absence of APP. Altogether, these results demonstrate a role for APP in venous, but not arterial, thrombosis.

### Platelet-associated APP controls fibrin formation through the intrinsic pathway

It is known that activation of blood coagulation and neutrophil-driven inflammatory processes are major triggers for venous thrombosis.<sup>37</sup> Because platelet APP contains a KPI domain, which acts as a serine protease inhibitor capable of affecting the activity of different coagulation factors in vitro, we searched for alterations of clot formation in APP-KO mice. Figure 5A shows that WT and APP-KO mice possess comparable amounts of circulating fibrinogen. Fibrin formation was then investigated by evaluating both the intrinsic and extrinsic pathways through APTT and PT assays, respectively. When PPP was used,

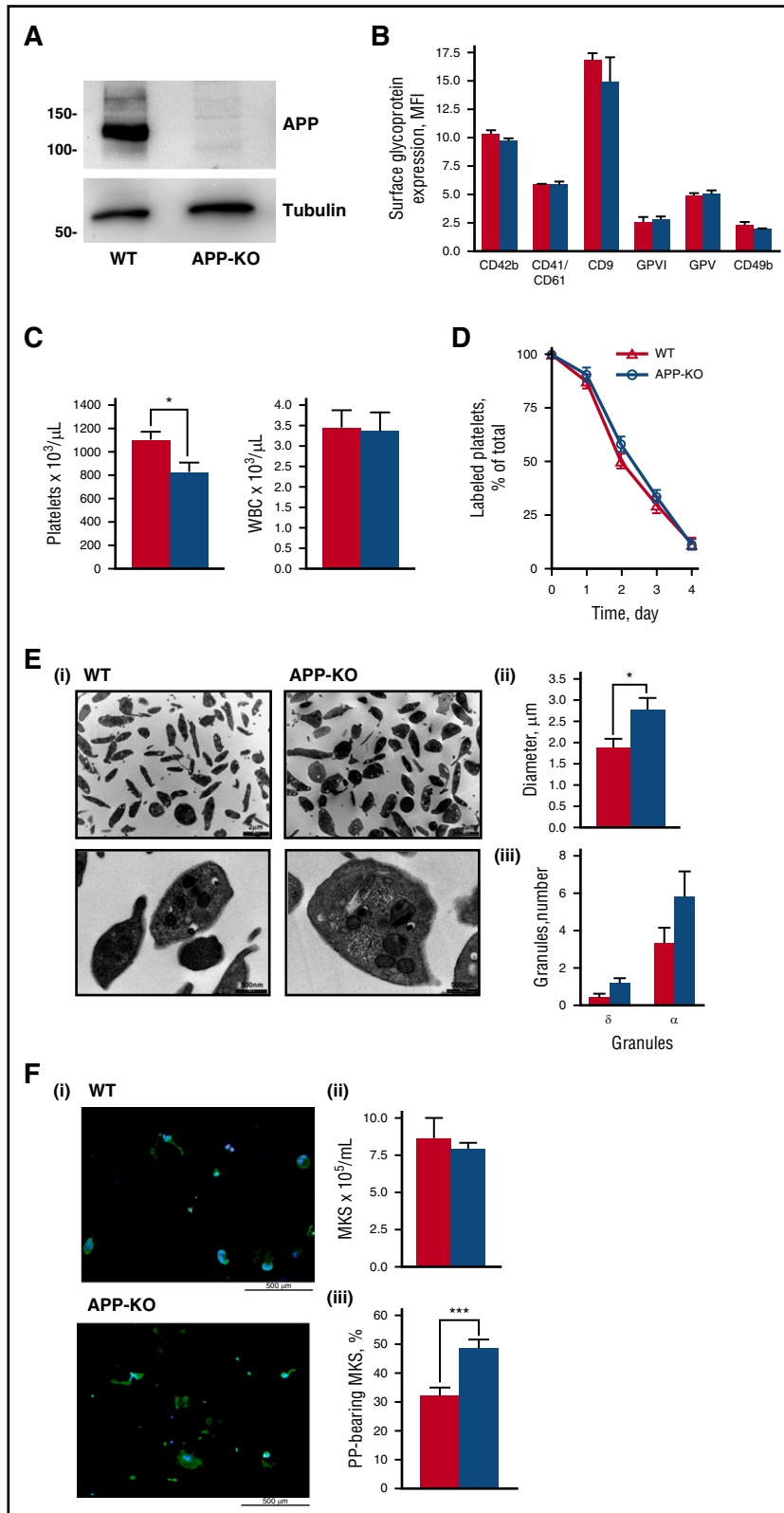


**Figure 1. Characterization of platelets from APP-KO mice.** In all the graphs, red bars refer to WT mice, and blue bars refer to APP-KO mice. Data are expressed as mean  $\pm$  SEM and have been obtained from 3 different experiments, unless otherwise specified. (A) Analysis of APP and tubulin (as control) expression in platelets from WT and APP-KO mice by immunoblotting with specific antibodies, as indicated. (B) Analysis of glycoprotein expression by flow cytometry. (C) Platelets and white blood cells count in whole blood. \* $P < .05$ . (D) Blood was withdrawn from WT and APP-KO mice at the indicated points after injection of AlexaFluor488-labeled antibodies to GPIX, and the fraction of labeled to unlabeled platelets was determined ( $n = 5$ ). (E) Electron microscopy analysis of platelet morphology. (i) Representative images at different magnitude (5600 $\times$ , upper; and 28 000 $\times$ , lower). Quantification of the mean platelet diameter and number of internal  $\alpha$  and dense ( $\delta$ ) granules is reported in (ii) and (iii), respectively. Data have been obtained from the analysis of 50 different platelets from 5 different slides. \* $P < .05$ . (F) Analysis of megakaryocytes and proplatelets formation. (i) Representative images of proplatelets forming megakaryocytes from WT and APP-KO mice on staining with anti-tubulin antibody (green) and with Hoechst (blue). Quantification of total megakaryocytes (MKS) and percentage of cells producing proplatelets (PP) is reported in (ii) and (iii), respectively. \*\*\* $P < .005$ .

no significant differences in the time required for clot formation were observed between WT and APP-KO mice (Figure 5B-C). However, when measurements were performed in the presence of platelets (using PRP), the APTT time was significantly shortened in the APP-KO mice (Figure 5E). In contrast, PT time still remained comparable in the 2

genotypes (Figure 5D). In reconstitution experiments, we found that addition of platelets from APP-KO mice to PPP from WT mice was able to significantly shorten the APTT compared with samples in which WT platelets were added to PPP from APP-KO mice (Figure 5F). These results indicate that APP expressed on the platelet surface negatively regulates

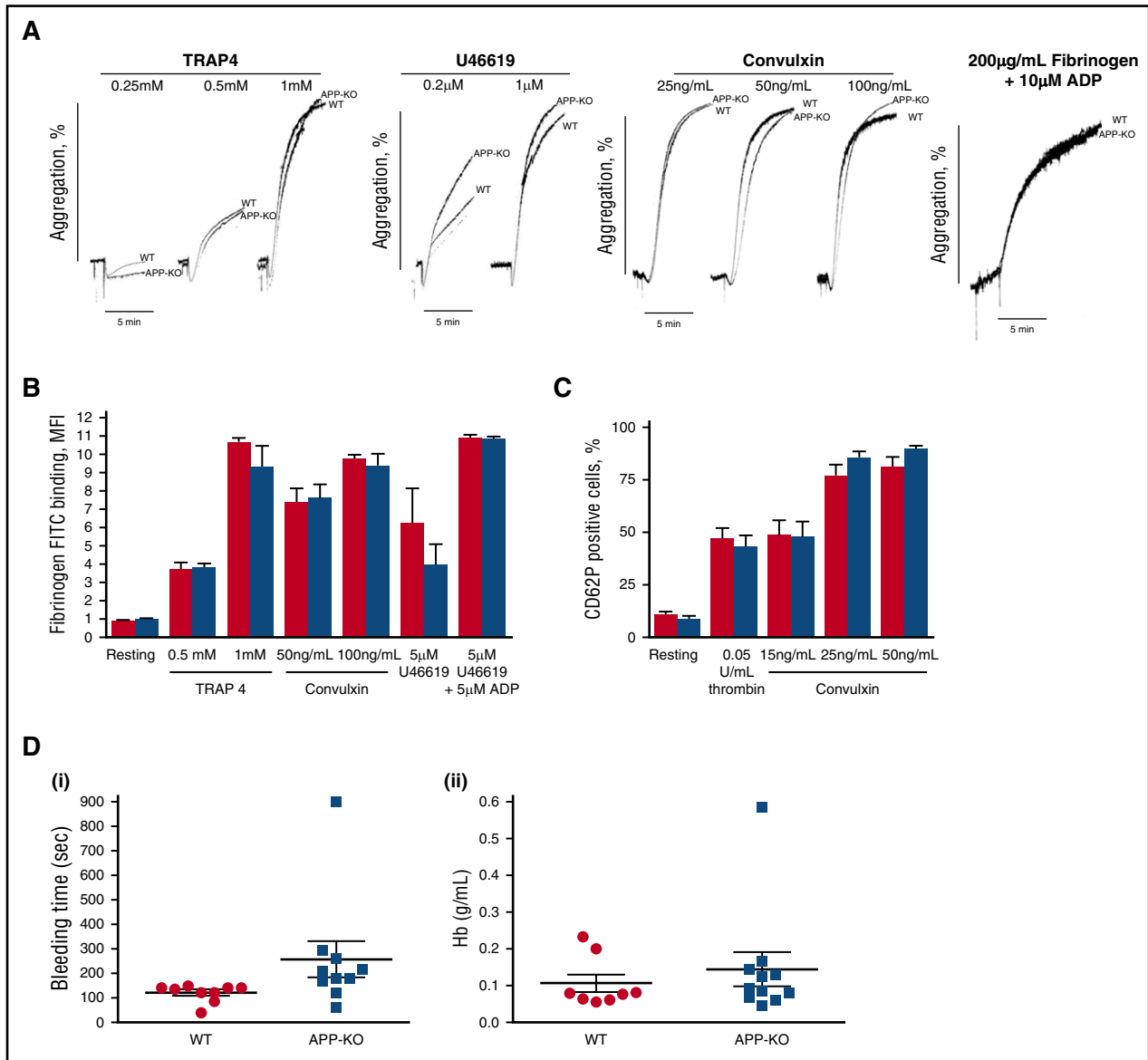


**Figure 2. Analysis of platelet function.** (A) Aggregation of washed platelets from WT and APP-KO mice induced by the indicated agonists. Aggregation induced by adenosine 5'-diphosphate (ADP) was measured on addition of purified fibrinogen, as indicated. (B-C) Flow cytometry analysis of agonist-induced integrin  $\alpha$ IIb $\beta$ 3 activation, measured as binding of fluorescein isothiocyanate-labeled fibrinogen (B) and granule secretion as P-selectin exposure (C). Red bars, WT platelets; blue bars, APP-deficient platelets. Results are the mean  $\pm$  SEM of 3 different experiments. (D) Tail bleeding time determined in groups of 10 mice for each genotype and expressed as time required for bleeding cessation (i) and amount of blood hemoglobin lost (ii). Each symbol represents 1 animal.

fibrin formation through the intrinsic pathway. To get insights into the possible target of APP in the coagulation cascade, we directly compared the activity of FXIIa and FXIa. FXIIa was reported to play an important role in the initiation of DVT,<sup>32</sup> whereas FXIa is the major substrate for the KPI inhibitory domain of APP.<sup>17</sup> Figure 5G shows that, when measured in PRP, FXIa activity, but not FXIIa activity, was significantly higher in the APP-KO mice.

**Enhanced NETs formation by neutrophils from APP-KO mice**

It has been documented that neutrophils play a role in propagating DVT mainly through the extrusion of procoagulant NETs.<sup>32,38</sup> Figure 6A shows that unstimulated neutrophils from APP-KO mice spontaneously protruded a much greater amount of NETs compared with WT cells. PMA stimulation strongly triggered NETs formation by WT neutrophils, but did not further significantly increase NETosis by

neutrophils from APP-KO mice. Interestingly, NETs formation by unstimulated neutrophils from APP-KO mice was comparable to that of PMA-stimulated WT cells. Although the expression of APP in murine neutrophils was hardly detectable by immunoblotting (data not shown), it is known that platelets regulate NETs formation. We found that both control and APP-deficient platelets were equally efficient in stimulating NETs formation by neutrophils from either WT or APP-KO mice (Figure 6B). Thus, platelets can stimulate neutrophils to extrude NETs, independent of APP expression. Nevertheless, we found that the number of circulating platelet-leukocyte aggregates in APP-KO mice was significantly higher than in WT control mice (Figure 6C), and stimulation with thrombin further increased the formation of these complexes in both genotypes (Figure 6C). To support the correlation between NETs formation and venous thrombosis, we performed histochemical



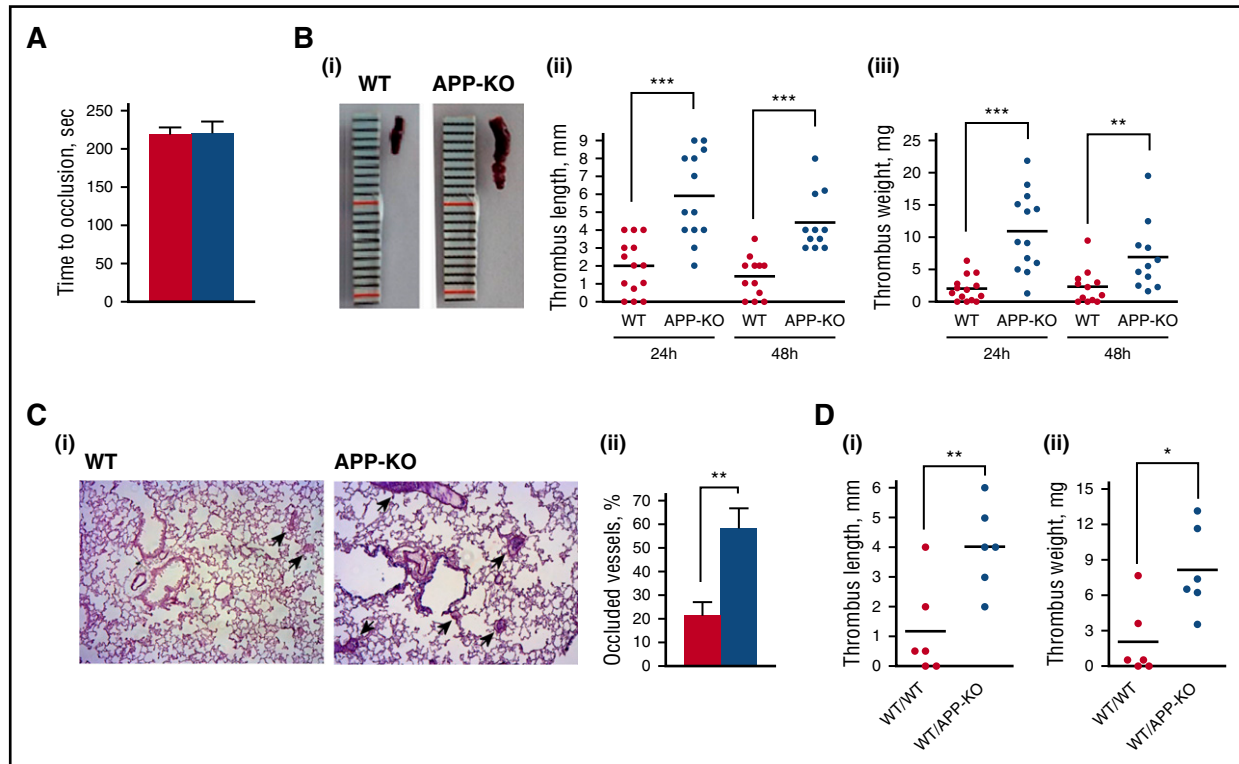


**Figure 3. Analysis of thrombus formation in vivo.** (A) Photochemical-induced arterial thrombosis assessed as time required for occlusion of femoral artery measured by laser Doppler in WT (red bars) and APP-KO (blue bars) mice. Data are the mean  $\pm$  SEM of measurements performed on 5 animals for both genotypes. (B) Analysis of deep vein thrombosis. Thrombus formation in the IVC was induced by vein ligation. Thrombi were extracted 24 or 48 hours after surgery. (i) Representative image showing the different size of thrombi from WT and APP-KO mice after 24 hours of ligation. Quantifications of thrombus length and weight at 24 and 48 hours are reported in (ii) and (iii), respectively.  $**P < .01$ ;  $***P < .005$ . (C) Analysis of thrombus embolization. (i) Staining of lung sections from WT or APP-KO with phosphotungstic acid-hematoxylin. Samples were prepared 48 hours on IVC ligation. Fibrin-occluded vessels are indicated by the arrows. (ii) Analysis of the percentage of occluded vessel observed in the 2 genotypes. Data are presented as mean  $\pm$  SEM.  $n = 5$ .  $**P < .01$ . (D) Comparison of venous thrombosis in WT mice transplanted with bone marrow cells from WT animals (WT/WT) and in WT mice transplanted with bone marrow cells from APP-KO mice (WT/APPKO). Thrombus length is reported in (i) and thrombus weight in (ii).  $*P < .05$ ;  $**P < .001$ .

analysis to visualize incorporation of NETs into the formed thrombi. Staining for 2 NETs-related markers, CRAMP and citrullinated histone H3, revealed a significantly stronger incorporation of NETs into venous thrombi from APP-KO compared with WT mice (Figure 6D). Altogether, these results indicate that the absence of APP leads to an increased constitutive interaction of platelets with neutrophils, associated with a stronger NETs formation.

## Discussion

In the present study, we have demonstrated a novel role for APP in the regulation of venous thromboembolism. In a model of flow restriction-induced DVT, we demonstrated that mice lacking APP develop significantly larger thrombi than control littermates. Moreover, in a

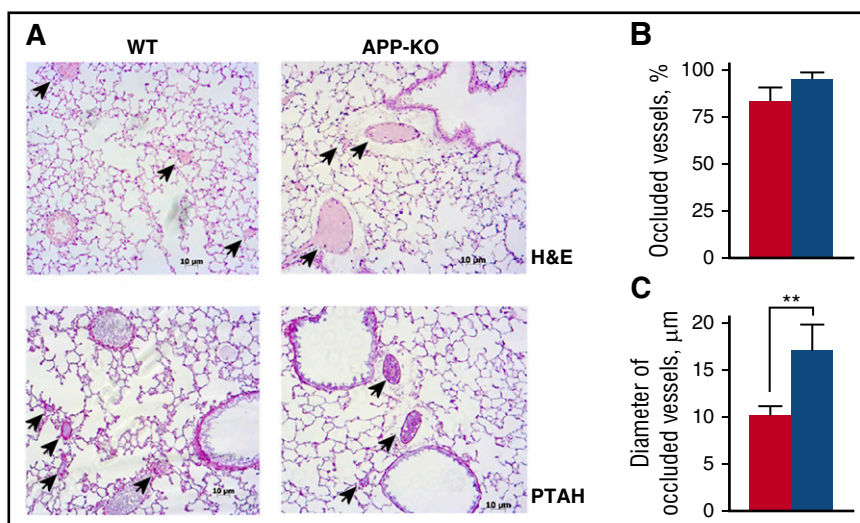


**Figure 4. Analysis of pulmonary thromboembolism.** (A) Representative lung histology images on staining with hematoxylin/eosin (H&E) and phosphotungstic acid-hematoxylin (PTAH). Arrows indicate occluded vessels. Quantification of the percentage of occluded vessels is reported in (B), and analysis of the mean diameter of occluded vessels is reported in (C). Data have been collected by examining 10 microscopic fields for each lung section, prepared from 5 different animals, and are presented as mean  $\pm$  SEM.  $**P < .01$ .

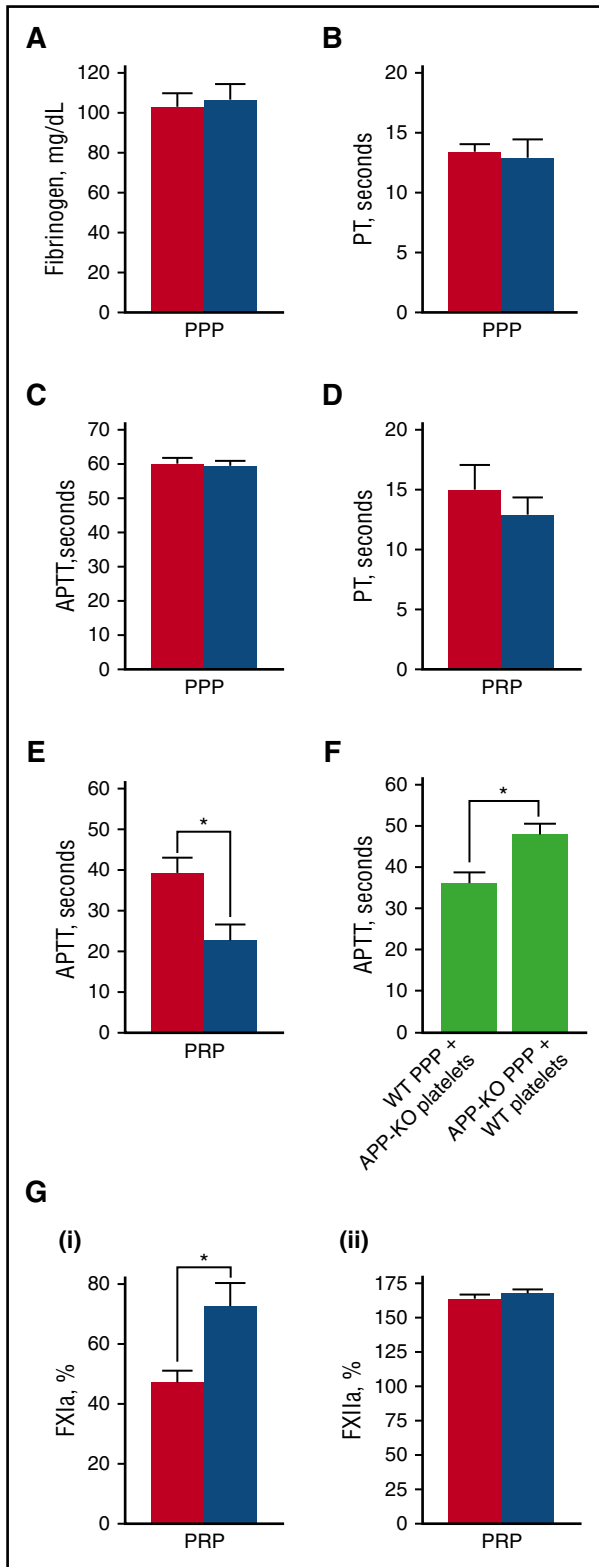


**Figure 5. Blood clotting assays.** In all panels, red bars refer to WT mice, and blue bars to APP-KO mice. Data are expressed as mean  $\pm$  SEM of 10 different determinations. Quantification of the level of plasma fibrinogen in the 2 genotypes is reported in (A). PT (B,D) and APTT (C,E) was measured in PPP (B-C) and PRP (D-E). \* $P < .05$ . (F) Measurement of APTT in reconstituted samples obtained by mixing PPP from 1 genotype with washed platelets from the other genotype, as indicated. \* $P < .05$ . (G) Quantification of the activity of FXIa (i) and FXIIa (ii) in PRP from WT and APP-KO mice. \* $P < .05$ .

pulmonary thromboembolism model, vessels with a significantly larger diameter were occluded in APP-KO mice compared with controls.

Circulating platelets contain high levels of APP. However, because of the implications of APP-derived A $\beta$  peptides in the onset and progression of Alzheimer disease, previous studies have focused mainly on the central nervous system. As a consequence, very little is known about the physiological function of the membrane-associated full-length APP as a platelet receptor and as a potential regulator of hemostasis and thrombosis. In line with this, APP-KO mice also have been mainly used for neurological and behavioral studies. Only a single previous study has documented a role for platelet APP in limiting cerebral thrombosis, evaluated in an intracerebral hemorrhage model as well as in a carotid artery thrombosis assay.<sup>21</sup>

In the present study, we addressed the function of APP in the peripheral circulation, where platelets differently contribute to both arterial and venous thrombosis, and we have demonstrated that in these vascular districts, the implication of APP differs from that described in the cerebral circulation. In fact, different from what was reported in the carotid artery,<sup>21</sup> we observed that photochemical-induced thrombosis in the femoral artery occurred normally in the absence of APP. Although the reason for this difference is unclear, this observation is in line with the notion that the response to specific thrombotic injuries may vary depending on the vascular site.<sup>39</sup> On the contrary, we observed for the first time that thrombosis in the IVC was significantly enhanced in the absence of APP. Moreover, APP-KO mice were more sensitive to developing pulmonary thromboembolism. Thus, in the peripheral circulation, APP regulates venous, rather than arterial, thrombosis. Importantly, formation of larger venous thrombi was also measured in chimeric mice on transplantation of bone marrow from APP-KO mice into WT animals, demonstrating the direct implication of APP in blood cells for the regulation of this process.

Arterial thrombosis is more dependent on platelet function than vein thrombosis, which mostly relies on the activation of the coagulation cascade. The normal arterial thrombosis in APP-KO mice is consistent with our observations that APP does not significantly regulate platelet function. No alterations of aggregation, secretion, and integrin  $\alpha$ IIb $\beta$ 3 inside-out activation in response to a wide panel of agonists were observed in APP-deficient platelets. Moreover, the absence of APP did not affect the tail bleeding time, indicating that the overall platelet-dependent hemostatic response is well preserved. Nevertheless, we observed a slight but significant reduction of the number of circulating platelets and an increase of the platelet diameter in APP-KO mice. Although the life span of APP-deficient platelets was normal, we found a greater percentage of bone marrow-derived megakaryocytes protruding proplatelets in APP-KO mice. How this can be related to the reduced number of circulating platelets remains to be clarified. It is possible, however, that dysregulated proplatelet formation leads to premature release of platelets in the bone marrow, thus resulting in a reduced number of cells reaching the circulation, a mechanism similar to that proposed for the MYH9-related macrothrombocytopenia.<sup>40</sup>

In our study, we documented significant alterations of clot formation in APP-KO mice. Different from the neuronal isoform, APP expressed in platelets carries a KPI domain, which is a potent inhibitor of serine proteases.<sup>9</sup> Purified or recombinant KPI domains containing APP fragments have been deeply characterized in vitro and found to potentially affect many coagulation factors, including FIXa, FXa, FVII:tissue factor complex, and particularly FXIa.<sup>17-20</sup> Because soluble truncated forms of APP are stored into platelet granules and platelet stimulation also promotes shedding of membrane APP,<sup>10,16</sup> platelets are a source of circulating KPI-containing APP fragments that are supposed to exert a tonic inhibitory action on clot formation.<sup>41</sup> Here, we showed that platelet-bound APP, rather than soluble fragments, exerts

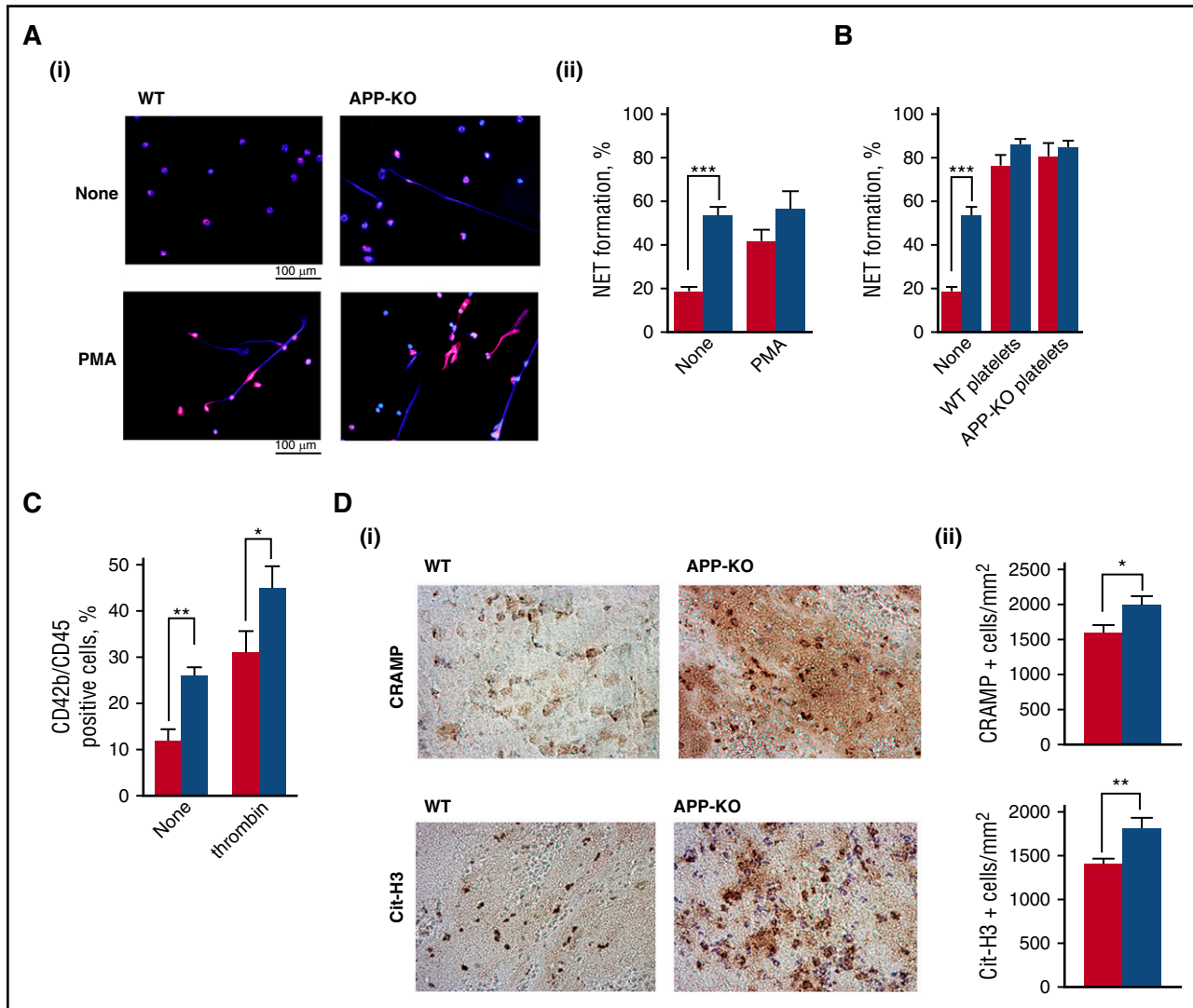


**Figure 6. Analysis of NETs formation.** In all the panels, red bars refer to WT mice, and blue bars to APP-KO mice. Data are expressed as mean  $\pm$  SEM of at least 5 different determinations. (A) NETs formation in purified neutrophils from WT and APP-KO mice was visualized by staining for DNA with Hoechst (blue) and for citrullinate Histone H3 (red). Representative images of resting and PMA-stimulated neutrophils are reported in (i), and quantification of the NETs formation expressed as percentage of neutrophils extruding NETs is reported in (ii). \*\*\* $P < .005$ . (B) Analysis of NETs formation induced by incubation of WT and APP-KO neutrophils with WT platelets, APP-deficient platelets, or no cells (none), as indicated in the bottom. (C) Flow cytometry analysis of circulating platelet-leukocyte aggregates in blood from WT and APP-KO mice untreated (none) or on stimulation with 0.5 U/mL thrombin, as indicated. \* $P < .05$ ; \*\* $P < .01$ . (D) Venous thrombi were isolated from WT and APP-KO mice 24 hours on IVC ligation, and stained for the NETs-related markers CRAMP and citrullinated histone H3 (Cit-H3), as indicated. (i) Some representative images, whereas (ii) reports the quantification of the positive cells counted from 5 positive stained fields. Results are reported as mean  $\pm$  SEM. \* $P < .05$ ; \*\* $P < .01$ .

an important inhibitory action on the coagulation cascade by targeting the intrinsic pathway, and thus regulating DVT. However, as APP can be rapidly metabolized on platelet activation, it cannot be ruled out that in the course of venous thrombosis, recruited platelets release APP fragments in the microenvironment, which may play a role as well. Even in this case, however, the involvement of platelet APP in the process is indispensable. We found that the intrinsic pathway of coagulation is affected in APP-KO mice, with some evidence that FXIa, but not FXIIa, both of which are implicated in DVT,<sup>32</sup> is a major target of platelet APP. Therefore, we propose that lack of APP in platelets accelerates clot formation through the intrinsic pathway, and this may be responsible for the formation of larger thrombi on vein flow restriction.

It is important to keep in mind that in addition to APP, platelets express, albeit at a lower level, the APP-like protein 2 (APLP2), which, as APP, contains a KPI domain.<sup>4,6</sup> Previous studies have documented that similar to APP, APLP2 also regulates cerebral thrombosis.<sup>42</sup> It is

therefore likely that APLP2 may also contribute to the regulation of clot formation and DVT, and that the consequence of APP deletion described in this study may be partially mitigated by the overlapping compensatory effect of APLP2. Further studies on APLP2-KO mice may be useful to characterize the specific contribution of APLP2 in hemostasis and thrombosis, but the clarification of the compensatory role of APP and APLP2 is hampered by the fact that APP/APLP2 double-KO mice die early after birth, for unknown reasons.<sup>43</sup>

It is well-known that, in addition to platelets, circulating neutrophils actively participate in the onset and propagation of DVT by promoting the activation of the coagulation cascade through the release of NETs.<sup>32,38</sup> Here we found that neutrophils from APP-KO mice released a higher amount of NETs than neutrophils from control animals, even in the absence of specific stimulation, and that an increased amount of NETs was incorporated into venous thrombi in APP-KO mice. Such a negative regulation of NETosis by APP was unexpected. Because



murine neutrophils express a very low amount of APP, if any, it is possible that the absence of APP in other circulating cells may regulate the ability of neutrophils to release NETs. In this scenario, platelets may play a role, as they are capable of stimulating NETosis. Although we could not detect any difference in NETs formation promoted by WT or APP-deficient platelets, we detected a significant greater number of platelet–leukocyte aggregates in APP-KO mice. It is possible, therefore, that APP negatively regulates platelet–leukocyte interaction, and that, in APP-KO mice, neutrophils can be stimulated to release NETs by a massive constitutive interaction with platelets. Certainly, the increased number of platelet–leukocyte aggregates in the circulation is indicative of a pro-inflammatory state related to the absence of APP, which, in turn, may be responsible for stimulated NETosis and predispose APP-KO mice to DVT. In this context, we have measured higher level of C-reactive protein in the plasma of APP-KO mice compared with controls (data not shown). It is also possible that increased NETosis in APP-KO mice may be related to dysregulation of some still-unidentified proteases, a possibility that deserves further investigation. Whatever the mechanism, however, our data indicate that the stronger release of NETs by neutrophils may represent an additional mechanism supporting the greater venous thrombosis in APP-KO mice.

In conclusion, our study outlines a novel role for APP in vivo and recognizes an important contribution in thromboembolism through multiple mechanisms, involving both coagulation factors and neutrophil activity. These results shed new light in the complexity of the mechanisms of DVT and may help understand previously uncharacterized pathological conditions.

## References

- Gandy S. The role of cerebral amyloid beta accumulation in common forms of Alzheimer disease. *J Clin Invest*. 2005;115(5):1121-1129.
- Thinakaran G, Koo EH. Amyloid precursor protein trafficking, processing, and function. *J Biol Chem*. 2008;283(44):29615-29619.
- Deyts C, Thinakaran G, Parent AT. APP receptor? To be or not to be. *Trends Pharmacol Sci*. 2016;37(5):390-411.
- Müller UC, Zheng H. Physiological functions of APP family proteins. *Cold Spring Harb Perspect Med*. 2012;2(2):a006288.
- Li QX, Berndt MC, Bush AI, et al. Membrane-associated forms of the beta A4 amyloid protein precursor of Alzheimer's disease in human platelet and brain: surface expression on the activated human platelet. *Blood*. 1994;84(1):133-142.
- Burkhardt JM, Vaudel M, Gambaryan S, et al. The first comprehensive and quantitative analysis of human platelet protein composition allows the comparative analysis of structural and functional pathways. *Blood*. 2012;120(15):e73-e82.
- Tanzi RE, McClatchey AI, Lamperti ED, Villa-Komaroff L, Gusella JF, Neve RL. Protease inhibitor domain encoded by an amyloid protein precursor mRNA associated with Alzheimer's disease. *Nature*. 1988;331(6156):528-530.
- Kitaguchi N, Takahashi Y, Tokushima Y, Shiojiri S, Ito H. Novel precursor of Alzheimer's disease amyloid protein shows protease inhibitory activity. *Nature*. 1988;331(6156):530-532.
- Van Nostrand WE, Wagner SL, Suzuki M, et al. Protease nexin-II, a potent antichymotrypsin, shows identity to amyloid beta-protein precursor. *Nature*. 1989;341(6242):546-549.
- Van Nostrand WE, Schmaier AH, Farrow JS, Cunningham DD. Protease nexin-II (amyloid beta-protein precursor): a platelet alpha-granule protein. *Science*. 1990;248(4956):745-748.
- Catricalà S, Torti M, Ricevuti G. Alzheimer disease and platelets: how's that relevant. *Immun Ageing*. 2012;9(1):20.
- Canobbio I, Abubaker AA, Visconte C, Torti M, Pula G. Role of amyloid peptides in vascular dysfunction and platelet dysregulation in Alzheimer's disease. *Front Cell Neurosci*. 2015;9:65.
- Sonkar VK, Kulkarni PP, Dash D. Amyloid  $\beta$  peptide stimulates platelet activation through RhoA-dependent modulation of actomyosin organization. *FASEB J*. 2014;28(4):1819-1829.
- Canobbio I, Guidetti GF, Oliviero B, et al. Amyloid  $\beta$ -peptide-dependent activation of human platelets: essential role for  $Ca^{2+}$  and ADP in aggregation and thrombus formation. *Biochem J*. 2014;462(3):513-523.
- Canobbio I, Catricalà S, Di Pasqua LG, et al. Immobilized amyloid  $\beta$  peptides support platelet adhesion and activation. *FEBS Lett*. 2013;587(16):2606-2611.
- Canobbio I, Catricalà S, Balduini C, Torti M. Calmodulin regulates the non-amyloidogenic metabolism of amyloid precursor protein in platelets. *Biochim Biophys Acta*. 2011;1813(3):500-506.
- Smith RP, Higuchi DA, Broze GJ Jr. Platelet coagulation factor XIa-inhibitor, a form of Alzheimer amyloid precursor protein. *Science*. 1990;248(4959):1126-1128.
- Schmaier AH, Dahl LD, Rozemuller AJ, et al. Protease nexin-2/amyloid beta protein precursor. A tight-binding inhibitor of coagulation factor IXa. *J Clin Invest*. 1993;92(5):2540-2545.
- Mahdi F, Van Nostrand WE, Schmaier AH. Protease nexin-2/amyloid beta protein precursor inhibits factor Xa in the prothrombinase complex. *J Biol Chem*. 1995;270(40):23468-23474.
- Mahdi F, Rehemtulla A, Van Nostrand WE, Bajaj SP, Schmaier AH. Protease nexin-2/Amyloid beta-protein precursor regulates factor VIIa and the factor VIIa-tissue factor complex. *Thromb Res*. 2000;99(3):267-276.
- Xu F, Davis J, Miao J, et al. Protease nexin-2/amyloid beta-protein precursor limits cerebral thrombosis. *Proc Natl Acad Sci USA*. 2005;102(50):18135-18140.
- Xu F, Previti ML, Van Nostrand WE. Increased severity of hemorrhage in transgenic mice expressing cerebral protease nexin-2/amyloid beta-protein precursor. *Stroke*. 2007;38(9):2598-2601.
- Müller U, Cristina N, Li ZW, et al. Behavioral and anatomical deficits in mice homozygous for a modified beta-amyloid precursor protein gene. *Cell*. 1994;79(5):755-765.
- Canobbio I, Visconte C, Oliviero B, et al. Increased platelet adhesion and thrombus formation in a mouse model of Alzheimer's disease. *Cell Signal*. 2016;28(12):1863-1871.
- Canobbio I, Cipolla L, Consonni A, et al. Impaired thrombin-induced platelet activation and thrombus formation in mice lacking the  $Ca^{2+}$ -dependent tyrosine kinase Pyk2. *Blood*. 2013;121(4):648-657.
- Stefanini L, Paul DS, Robledo RF, et al. RASA3 is a critical inhibitor of RAP1-dependent platelet activation. *J Clin Invest*. 2015;125(4):1419-1432.
- Momi S, Falcinelli E, Giannini S, et al. Loss of matrix metalloproteinase 2 in platelets reduces arterial thrombosis in vivo. *J Exp Med*. 2009;206(11):2365-2379.
- Bolliger D, Szlam F, Suzuki N, Matsushita T, Tanaka KA. Heterozygous antithrombin deficiency improves in vivo haemostasis in factor VIII-deficient mice. *Thromb Haemost*. 2010;103(6):1233-1238.
- Gresele P, Momi S, Berrettini M, et al. Activated human protein C prevents thrombin-induced thromboembolism in mice. Evidence that activated protein c reduces intravascular fibrin accumulation through the inhibition of additional

## Acknowledgments

The authors thank Ulrike Muller (Institute for Pharmacy and Molecular Biotechnology, University of Heidelberg, Germany) for the APP-KO mice, and Annamaria Mezzasoma (Department of Medicine, Section of Internal and Cardiovascular Medicine, University of Perugia, Perugia, Italy) for help with electron microscopy analysis.

## Authorship

Contribution: I.C. designed and performed experiments, analyzed data, and wrote the manuscript; C.V. designed and performed experiments, analyzed data, and edited the manuscript; S.M. performed experiments, analyzed data, and edited the manuscript; G.F.G., M.Z., J.C., and E.F. performed experiments and analyzed data; P.G. analyzed data and edited the manuscript; and M.T. designed research, analyzed data, and wrote the manuscript.

Conflict-of-interest disclosure: The authors declare no competing financial interests.

Correspondence: Mauro Torti, Department of Biology and Biotechnology, University of Pavia, via Bassi 21, 27100 Pavia, Italy; e-mail: mtorti@unipv.it.

- thrombin generation. *J Clin Invest*. 1998;101(3):667-676.
30. Momi S, Caracchini R, Falcinelli E, Evangelista S, Gresele P. Stimulation of platelet nitric oxide production by nebivolol prevents thrombosis. *Arterioscler Thromb Vasc Biol*. 2014;34(4):820-829.
  31. Brill A, Fuchs TA, Chauhan AK, et al. von Willebrand factor-mediated platelet adhesion is critical for deep vein thrombosis in mouse models. *Blood*. 2011;117(4):1400-1407.
  32. von Brühl ML, Stark K, Steinhart A, et al. Monocytes, neutrophils, and platelets cooperate to initiate and propagate venous thrombosis in mice in vivo. *J Exp Med*. 2012;209(4):819-835.
  33. Momi S, Nasimi M, Colucci M, Nenci GG, Gresele P. Low molecular weight heparins prevent thrombin-induced thrombo-embolism in mice despite low anti-thrombin activity. Evidence that the inhibition of feed-back activation of thrombin generation confers safety advantages over direct thrombin inhibition. *Haematologica*. 2001;86(3):297-302.
  34. Mócsai A, Zhang H, Jakus Z, Kitaura J, Kawakami T, Lowell CA. G-protein-coupled receptor signaling in Syk-deficient neutrophils and mast cells. *Blood*. 2003;101(10):4155-4163.
  35. Lewis HD, Liddle J, Coote JE, et al. Inhibition of PAD4 activity is sufficient to disrupt mouse and human NET formation. *Nat Chem Biol*. 2015;11(3):189-191.
  36. Knight JS, Zhao W, Luo W, et al. Peptidylarginine deiminase inhibition is immunomodulatory and vasculoprotective in murine lupus. *J Clin Invest*. 2013;123(7):2981-2993.
  37. Swystun LL, Liaw PC. The role of leukocytes in thrombosis. *Blood*. 2016;128(6):753-762.
  38. Kimball AS, Obi AT, Diaz JA, Henke PK. The emerging role of NETs in venous thrombosis and immunothrombosis. *Front Immunol*. 2016;7:236.
  39. Westrick RJ, Winn ME, Eitzman DT. Murine models of vascular thrombosis (Eitzman series). *Arterioscler Thromb Vasc Biol*. 2007;27(10):2079-2093.
  40. Chen Z, Shivdasani RA. Regulation of platelet biogenesis: insights from the May-Hegglin anomaly and other MYH9-related disorders. *J Thromb Haemost*. 2009;7(Suppl 1):272-276.
  41. Van Nostrand WE. The influence of the amyloid  $\beta$ -protein and its precursor in modulating cerebral hemostasis. *Biochim Biophys Acta*. 2016;1862(5):1018-1026.
  42. Xu F, Previti ML, Nieman MT, Davis J, Schmaier AH, Van Nostrand WE. AbetaPP/APLP2 family of Kunitz serine proteinase inhibitors regulate cerebral thrombosis. *J Neurosci*. 2009;29(17):5666-5670.
  43. von Koch CS, Zheng H, Chen H, et al. Generation of APLP2 KO mice and early postnatal lethality in APLP2/APP double KO mice. *Neurobiol Aging*. 1997;18(6):661-669.